Letters in Applied NanoBioScience
Open-Access Journal (ISSN: 2284-6808)

Article
Volume 13, Issue 4, 2024, 169
https://doi.org/10.33263/LIANBS134.169

Annealing Time Effect on the Structural, Optical, and Electrical Characteristics of Titanium Dioxide Thin Films

Neha Sharma [1], Rajesh Kumar [1,*]

[1] Department of Physics, Lovely Professional University, Phagwara, Punjab-144401, India
* Correspondence: rajesh.12236@lpu.co.in;

Scopus Author ID 57198684609

Received: 14.09.2023; Accepted: 13.05.2024; Published: 25.08.2024

Abstract: Using the sol-gel spin coating method, TiO_2 thin films are fabricated and annealed at 500°C for different annealing times, i.e., 1 hour, 2 hours, 3 hours, and 4 hours. Annealing time is one of the parameters that influence the properties of thin films. This work investigates the effect of annealing time on the structural, optical, and electrical properties of TiO_2 films. All the films have a single anatase crystalline phase. The crystallite size increases with annealing time from 1 hour to 2 hours and then decreases. A decrease in band gap is observed due to an increase in grain size. The film annealed for 4 hours has the least resistivity.

Keywords: sol-gel; annealing time; thin films; optoelectronic properties.

1. Introduction

Titanium dioxide has been of great interest to researchers for a long time due to its optical and electrical properties, such as its chemical stability, high dielectric constant, and transparency. It is a metal oxide semiconductor with a wide range of applications, such as in solar cells, antireflective coatings, photocatalysis, and gas sensors [1–9]. Moreover, its high refractive index and low absorption can be used in optical devices such as optical fibers, waveguides, and amplifiers. Furthermore, titanium dioxide is also used in sputtering processes, where its high melting point and low thermal conductivity are beneficial. Additionally, it can be used in various semiconductor applications, such as in transistors, photodetectors, and diodes [10–14]. It is also used in medical applications, such as photodynamic therapy, drug delivery systems, and tissue scaffolds [15–18]. All these properties make titanium dioxide a versatile material for many different applications [19–29]. TiO_2 can be fabricated in various forms, such as nanowires, nanotubes, nanoparticles, nanosheets, etc [30–38]. TiO_2 thin films are highly sought after for their superior properties compared to their bulk material counterparts. This is because thin films enhance the material's physical, chemical, and electrical properties. In order to fabricate TiO_2 thin films, there are a number of techniques available, such as Chemical Vapor Deposition (CVD), Spray Pyrolysis, Atomic Layer Deposition (ALD), Sputtering, Electron Beam Evaporation, and Spin Coating [39–49]. Sol-gel is a versatile and cost-effective method for synthesizing high-purity homogeneous thin films. The spin coating technique allows the fabrication of uniform films on large areas, flexible substrates, and with minimal instrumentation. This method is especially beneficial in microelectronics, optics, and photonics applications.

Film properties such as crystallite size, band gap, electric conductivity, and surface morphology are closely linked to parameters such as thickness, molarity of the solution, pH of the solution, spin speed, and annealing temperature [26-31]. By understanding the influence of parameters on film properties, it is possible to optimize the production process in order to produce films with desired characteristics. This can lead to improved performance in applications such as solar cells, displays, and batteries. The annealing time is an important factor when considering the properties of TiO_2 films. While there have been some investigations into the effect of annealing time on the optical and structural properties of TiO_2 films, there is still much to be explored in this area. It is known that the annealing time of the TiO_2 film can alter the structural properties, such as the crystallinity and grain size, as well as the optical properties, such as the absorption coefficient and refractive index. Furthermore, the annealing time can also affect the electrical properties of the TiO_2 film, such as the sheet resistance.

This work focuses on optimizing the annealing time of TiO_2 thin films with a range of 1, 2, 3, and 4 hours and annealing temperature of 500°C. The effects of the annealing process on the optical, structural, and electrical properties of the TiO_2 films are also examined. Various parameters, such as crystallinity, transmittance, optical band gap, and electrical resistivity, are studied.

2. Materials and Methods

Titanium Isopropoxide (TTIP) is dissolved in the mixture of diethylene glycol and ethanol in the ratio of 1:1:20 to obtain the coating TiO_2 sol, as shown in Figure 1. The solution is stirred at room temperature for 30 minutes. The reaction between the TTIP and ethanol is a process of hydrolysis and condensation, as given in equations (1) and (2). The films are prepared using the spin coating technique. The solution is deposited onto the glass substrate. The glass substrate is cleaned with methanol, acetone, and distilled water and is dried for a few minutes. The substrate is spun at 1500 rpm for 15 sec. The films are preheated at 100°C for 5 minutes after every layer deposition. Finally, the films are annealed at 500°C for 1 hour, 2 hours, 3 hours, and 4 hours.

$$(Ti(OC_3H_7)_4) + 4C_2H_5OH \xrightarrow{\text{Hydrolysis}} Ti(OH)_4 + 4C_2H_5OH \quad (1)$$

$$Ti(OH)_4 \xrightarrow{\text{Condensation}} TiO_2.x\,H_2O \quad (2)$$

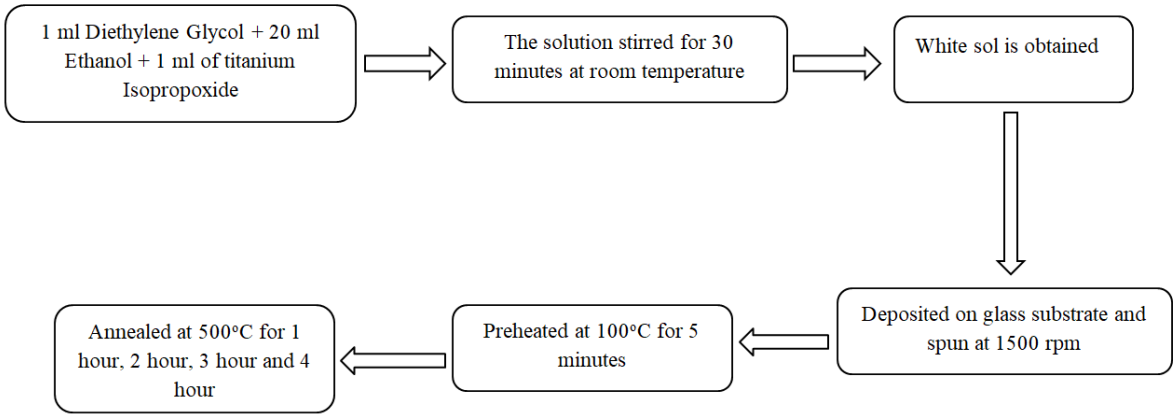

Figure 1. Preparation of the TiO_2 thin films annealed at different annealing times.

The structural, optical, and electrical properties of titanium dioxide thin films are investigated using X-ray diffraction (Bruker D8 Advance), UV-visible spectroscopy

(Shimadzu UV-1900 i), and the Two-point probe method. The films' crystallite size, band gap, and resistivity are analyzed using origin software.

3. Results and Discussion

3.1. Structural study.

Figure 2 shows the XRD pattern of the films annealed at 500°C for 1 hour, 2 hours, 3 hours, and 4 hours. The peaks correspond to the planes (101), (004), (200), (105), (211), (204) are at 25°, 38°, 48°, 54°, 55°, 63°. The obtained peaks are similar to the JCPDS file no. 21-1276. The XRD reveals that the films are crystalline and have an anatase phase of TiO_2. It can also be seen that the peak shifts towards the lower angle when the annealing hour increases; this is attributed to the decrease in the crystallinity of the films. The crystallite sizes of the films are estimated using the Scherrer formula. [32]

$$D = \frac{0.96 \times \lambda}{\beta \cos \theta} \quad (3)$$

Where λ is the X-ray radiations, β is the FWHM, and θ is the diffraction angle. The lattice strain (∈) and dislocation density (δ) are estimated by using the relation [50]:

$$\in = \frac{\beta \cos\theta}{4 \sin\theta} \quad (4)$$

$$\delta = \frac{1}{D^2} \quad (5)$$

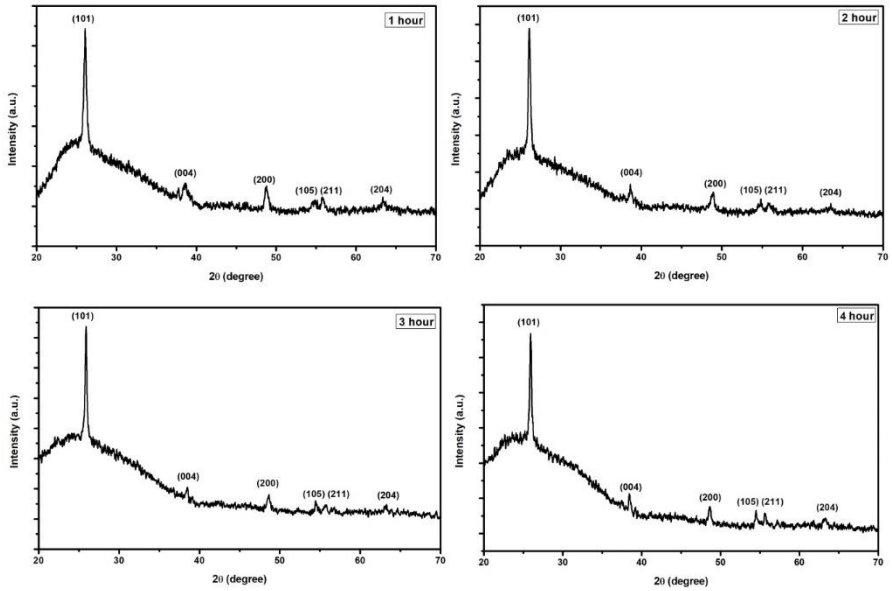

Figure 2. The XRD pattern of the films annealed for different annealing times.

The obtained results are presented in Table 1, though it can be seen that the TiO_2 thin film annealed for 2 hours has maximum crystallite size and minimum strain. The crystallite size increases for the films annealed for 1 hour and 2 hours because the higher the crystal growth, the higher the surface has convexity, reducing the lattice mismatch. Further, an increase in annealing time reduces the crystallite size. This may be due to the strain and interstitial defects [33]. It was also observed that the dislocation density decreases as the annealing time increases from 1 hour to 2 hours. It increases as the annealing time further increases from 2 hours. Thus, increased annealing temperature can cause lattice distortion and reduced crystallite size.

Table 1. The table shows the variation of crystallite size, strain, and dislocation density of TiO_2 thin films with annealing time.

Annealing time	Peaks (hkl)	2θ (°)	FWHM β (radian)	D (nm)	Strain ($\varepsilon \times 10^{-2}$)	Dislocation density (10^{-3}) (lines m^{-2})
1 hour	(101)	26.06	0.01155	13.14	1.248	5.79
2 hour	(101)	26.10	0.00861	17.63	0.928	3.21
3 hour	(101)	25.89	0.00981	15.46	1.067	4.18
4 hour	(101)	25.91	0.01223	12.41	1.329	6.40

3.2. Optical properties.

The optical properties of the TiO_2 thin films annealed at different annealing times are examined by UV-Vis spectroscopy with the range 1100 nm – 200 nm. The band gaps of the films are determined by using the Tauc equation [33]:

$$\alpha h\nu = \beta(h\nu - Eg)^m \quad (4)$$

Where α is the absorption coefficient, $h\nu$ is the energy, Eg is the band gap, and m is the indirect or direct transition.

Figure 3 shows the band gap of the films with annealing times of 1 hour, 2 hours, 3 hours, and 4 hours. The band gap of the films decreases with an increase in annealing time. This decrease in band gap is the result of larger grain size. The indirect band gap values for the thin films annealed at 500°C for 1 hour, 2 hours, 3 hours, and 4 hours are 3.67 eV, 3.57 eV, 3.53 eV, and 3.47 eV, respectively.

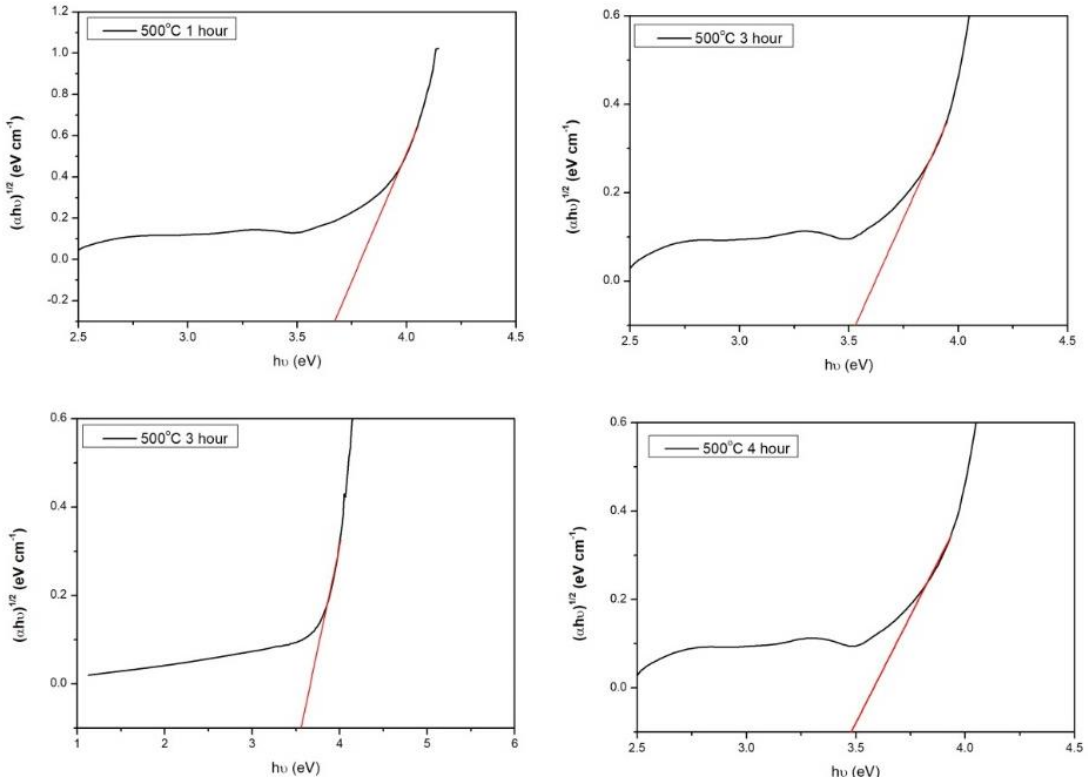

Figure 3. The indirect band gap of the TiO_2 thin films annealed with different annealing times.

3.3. Electrical properties.

The electrical conductivity of the TiO_2 thin films is measured using the two-point probe method. The I-V characteristics of the films examined keep the temperature constant at room temperature. Figure 4 shows that as the voltage rises from -20 V to 20 V, the current increases linearly. This shows that the contacts deposited on the films have ohmic behavior. Further, the

resistivities of the films are measured by keeping the voltage constant at 20 V, and variations of the current with respect to the temperature are measured. The resistivity of the films is calculated using the equation:

$$\rho = R\frac{A}{l} \quad (5)$$

$$\sigma = \frac{1}{\rho} \quad (6)$$

Where ρ is the resistivity, R is the resistance, A is the area of the films, l is the thickness of the films, and σ is the conductivity of the films.

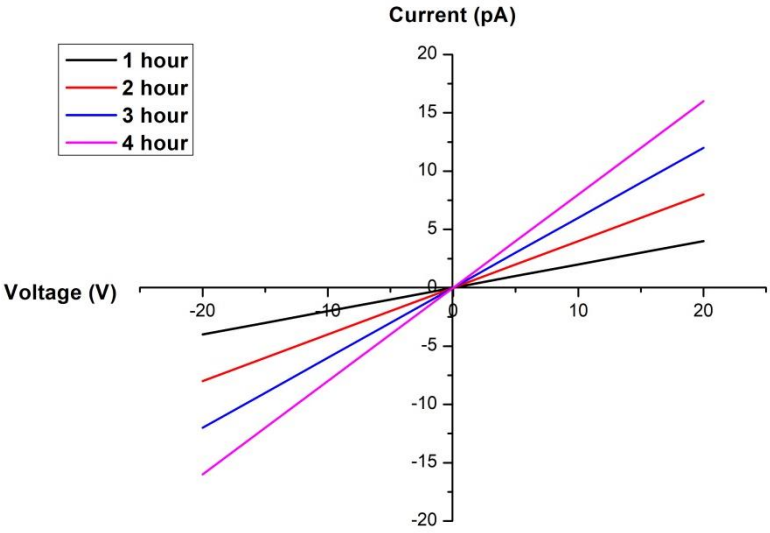

Figure 4. I-V characteristics of the TiO_2 thin films.

From the calculations, we observed that the resistivity of the samples decreased as the annealing time increased. This decrease was attributed to the excess charge carriers and more flow of electrons from one particle to another. The film annealed for 4 hours has the least resistivity. The resistivity of the thin films annealed for 1 hour, 2 hours, 3 hours, and 4 hours were 3.47×10^{14} Ωcm, 2.66×10^{14} Ωcm, 1.34×10^{14} Ωcm, 1.09×10^{14} Ωcm, respectively.

4. Conclusions

The TiO_2 thin films were synthesized using the sol-gel spin coating technique on a glass substrate. The films were annealed at 500°C for 1 hour, 2 hours, 3 hours, and 4 hours. The obtained results showed that the films show good crystallinity and have a tetragonal anatase phase. The band gap of the films was 3.67 eV, 3.57 eV, 3.53 eV, and 3.47 eV. The resistivity of the samples decreases with an increase in the annealing time. The films can be used for gas-sensing applications.

Funding

The authors declare that no funds or grants were received during this work.

Acknowledgments

Presented in 4th International Conference on "Recent Advances in Fundamental and Applied Sciences" (RAFAS-2023)" on March 24-25, 2023, Organized by the School of Chemical Engineering and Physical Sciences, Lovely Professional University, Punjab, India.

Conflicts of Interest

The authors have no competing interests to declare that are relevant to the content of this article.

References

1. Upadhyay, G.K.; Kumar, V.; Purohit, L.P. Optimized CdO:TiO_2 nanocomposites for heterojunction solar cell applications. *J. Alloys Compd.* **2021**, *856*, 157453, https://doi.org/10.1016/j.jallcom.2020.157453.
2. Kailasam, S.; Vijayan, R.A.; Amirthaganesan, D.; Srinath, S.; Viswanathan, V.; Masilamani, S.; Krishnamoorthy, P.; Varadharajaperumal, M. Accuracy of Contact Resistivity Measurements for Electron-Selective Titanium Oxide Contacts in n-Type c-Si Solar Cell. *IEEE J. Photovoltaics* **2021**, *11*, 613–619, https://doi.org/10.1109/JPHOTOV.2021.3056665.
3. Thangamani, G.J.; Pasha, S.K.K. Titanium dioxide (TiO_2) nanoparticles reinforced polyvinyl formal (PVF) nanocomposites as chemiresistive gas sensor for sulfur dioxide (SO_2) monitoring. *Chemosphere* **2021**, *275*, 129960, https://doi.org/10.1016/j.chemosphere.2021.129960.
4. Nunes Simonetti, E.A.; Cardoso de Oliveira, T.; Enrico do Carmo Machado, Á.; Coutinho Silva, A.A.; Silva dos Santos, A.; de Simone Cividanes, L. TiO_2 as a gas sensor: The novel carbon structures and noble metals as new elements for enhancing sensitivity – A review. *Ceram. Int.* **2021**, *47*, 17844–17876, https://doi.org/10.1016/j.ceramint.2021.03.189.
5. Waghchaure, R.H.; Koli, P.B.; Adole, V.A.; Pawar, T.B.; Jagdale, B.S. Transition metals Fe^{3+}, Ni^{2+} modified titanium dioxide (TiO_2) film sensors fabricated by CPT method to sense some toxic environmental pollutant gases. *J. Indian Chem. Soc.* **2021**, *98*, 100126, https://doi.org/10.1016/j.jics.2021.100126.
6. Nabi, I.; Bacha, A.-U.-R.; Ahmad, F.; Zhang, L. Application of titanium dioxide for the photocatalytic degradation of macro- and micro-plastics: A review. *J. Environ. Chem. Eng.* **2021**, *9*, 105964, https://doi.org/10.1016/j.jece.2021.105964.
7. Díaz-Sánchez, M.; Reñones, P.; Mena-Palomo, I.; López-Collazo, E.; Fresno, F.; Oropeza, F.E.; Prashar, S.; de la Peña O'Shea, V.A.; Gómez-Ruiz, S. Ionic liquid-assisted synthesis of F-doped titanium dioxide nanomaterials with high surface area for multi-functional catalytic and photocatalytic applications. *Appl. Catal. A Gen.* **2021**, *613*, 118029, https://doi.org/10.1016/j.apcata.2021.118029.
8. Natarajan, T.S.; Mozhiarasi, V.; Tayade, R.J. Nitrogen Doped Titanium Dioxide (N-TiO_2): Synopsis of Synthesis Methodologies, Doping Mechanisms, Property Evaluation and Visible Light Photocatalytic Applications. *Photochem* **2021**, *1*, 371–410, https://doi.org/10.3390/photochem1030024.
9. Abu-Shamleh, A.; Alzubi, H.; Alajlouni, A. Optimization of antireflective coatings with nanostructured TiO_2 for GaAs solar cells. *Photonics Nanostructures Fundam. Appl.* **2021**, *43*, 100862, https://doi.org/10.1016/j.photonics.2020.100862.
10. Ghosh, C.; Dey, A.; Biswas, I.; Gupta, R.K.; Yadav, V.S.; Yadav, A.; Yadav, N.; Zheng, H.; Henini, M.; Mondal, A. CuO–TiO_2 based self-powered broad band photodetector. *Nano Mater. Sci.* **2024**, *6*, 345-354, https://doi.org/10.1016/j.nanoms.2023.11.003.
11. Jasim, A.S.; Salman, O.N. Hydrothermally native defect induced transparent p-n TiO_2 homojunction diode. *Opt. Quantum Electron.* **2023**, *55*, 702, https://doi.org/10.1007/s11082-023-04984-6.
12. Agrohiya, S.; Kumar, V.; Rawal, I.; Dahiya, S.; Goyal, P.K.; Kumar, V.; Punia, R. Fabrication of n-TiO_2/p-Si Photo-Diodes for Self-Powered Fast Ultraviolet Photodetectors. *Silicon* **2022**, *14*, 11891–11901, https://doi.org/10.1007/s12633-022-01913-2.
13. Algadi, H.; Ren, J.; Alqarni, A. Solution-processed nitrogen-doped graphene quantum dots/perovskite composite heterojunction for boosting performance of anatase titanium dioxide (TiO_2)-based UV photodetector. *Adv. Compos. Hybrid Mater.* **2023**, *6*, 86, https://doi.org/10.1007/s42114-023-00667-8.
14. Alim, A.A.; Roslan, R.; Nadzirah, S.; Saidi, L.K.; Menon, P.S.; Aziah, I.; Chang Fu, D.; Sulaiman, S.A.; Abdul Murad, N.A.; Hamzah, A.A. Geometrical Characterisation of TiO_2-rGO Field-Effect Transistor as a Platform for Biosensing Applications. *Micromachines* **2023**, *14*, 1664, https://doi.org/10.3390/mi14091664.
15. Ramachandran, P.; Khor, B.-K.; Lee, C.Y.; Doong, R.-A.; Oon, C.E.; Thanh, N.T.K.; Lee, H.L. N-Doped Graphene Quantum Dots/Titanium Dioxide Nanocomposites: A Study of ROS-Forming Mechanisms, Cytotoxicity and Photodynamic Therapy. *Biomedicines* **2022**, *10*, 421, https://doi.org/10.3390/biomedicines10020421.
16. Zhang, T.; Liu, N.; Xie, C.; Xiao, X. Self-trigger and on-demand drug delivery system based on TiO_2 nanotube arrays and its drug release behaviour. *Micro Nano Lett.* **2023**, *18*, e12173,

https://doi.org/10.1049/mna2.12173.
17. Wang, P.; Zhang, L.; Zhang, Z.; Wang, S.; Yao, C. Influence of Parameters on Photodynamic Therapy of Au@TiO_2–HMME Core-Shell Nanostructures. *Nanomaterials* **2022**, *12*, 1358, https://doi.org/10.3390/nano12081358.
18. Dianová, L.; Tirpák, F.; Halo, M.; Slanina, T.; Massányi, M.; Stawarz, R.; Formicki, G.; Madeddu, R.; Massányi, P. Effects of Selected Metal Nanoparticles (Ag, ZnO, TiO_2) on the Structure and Function of Reproductive Organs. *Toxics* **2022**, *10*, 459, https://doi.org/10.3390/toxics10080459.
19. Velasco-Hernández, A.; Esparza-Muñoz, R.A.; de Moure-Flores, F.J.; Santos-Cruz, J.; Mayén-Hernández, S.A. Synthesis and characterization of graphene oxide - TiO_2 thin films by sol-gel for photocatalytic applications. *Mater. Sci. Semicond. Process.* **2020**, *114*, 105082, https://doi.org/10.1016/j.mssp.2020.105082.
20. AL-Shomar, S.M. Synthesis and characterization of Eu^{3+} doped TiO_2 thin films deposited by spray pyrolysis technique for photocatalytic application. *Mater. Res. Express.* **2021**, *8*, 026402, https://doi.org/10.1088/2053-1591/abe315.
21. Mokrushin, A.S.; Simonenko, E.P.; Simonenko, N.P.; Akkuleva, K.T.; Antipov, V.V.; Zaharova, N.V.; Malygin, A.A.; Bukunov, K.A.; Sevastyanov, V.G.; Kuznetsov, N.T. Oxygen detection using nanostructured TiO_2 thin films obtained by the molecular layering method. *Appl. Surf. Sci.* **2019**, *463*, 197-202, https://doi.org/10.1016/j.apsusc.2018.08.208.
22. Khan, M.I.; Mehmood, B.; Mustafa, G.M.; Humaiyoun, K.; Alwadai, N.; Almuqrin, A.H.; Albalawi, H.; Iqbal, M. Effect of silver (Ag) ions irradiation on the structural, optical and photovoltaic properties of Mn doped TiO_2 thin films based dye sensitized solar cells. *Ceram. Int.* **2021**, *47*, 15801-15806, https://doi.org/10.1016/j.ceramint.2021.02.152.
23. Fu, G.; Cho, E.J.; Luo, X.; Cha, J.; Kim, J.H.; Lee, H.W.; Kim, S.H. Enhanced light harvesting in panchromatic double dye-sensitized solar cells incorporated with bilayered TiO_2 thin film-based photoelectrodes. *Sol. Energy* **2021**, *218*, 346-353, https://doi.org/10.1016/j.solener.2021.03.011.
24. Purcar, V.; Rădiţoiu, V.; Dumitru, A.; Nicolae, C.-A.; Frone, A.N.; Anastasescu, M.; Rădiţoiu, A.; Raduly, M.F.; Gabor, R.A.; Căprărescu, S. Antireflective coating based on TiO_2 nanoparticles modified with coupling agents via acid-catalyzed sol-gel method. *Appl. Surf. Sci.* **2019**, *487*, 819-824, https://doi.org/10.1016/j.apsusc.2019.02.256.
25. Khan, S.B.; Zhang, Z.; Lee, S.L. Single component: Bilayer TiO_2 as a durable antireflective coating. *J. Alloys Compd.* **2020**, *834*, 155137, https://doi.org/10.1016/j.jallcom.2020.155137.
26. Mammeri, A.; Bouachiba, Y.; Bouabellou, A.; Serrar, H.; Laggoune, K.; Sekhri, I.; Taabouche, A.; Rahal, B.; Boulkra, M.; Nezzari, H. Optogeometric Study of Multimode Tio_2 Waveguide Thin Films Elaborated by Reactive Magnetron Sputtering. *Phys. B: Condens. Matter*. **2022**, *641*, 414059, https://doi.org/10.2139/ssrn.4022367.
27. Adewinbi, S.A.; Buremoh, W.; Owoeye, V.A.; Ajayeoba, Y.A.; Salau, A.O.; Busari, H.K.; Tijani, M.A.; Taleatu, B.A. Preparation and characterization of TiO_2 thin film electrode for optoelectronic and energy storage Potentials: Effects of Co incorporation. *Chem. Phys. Lett.* **2021**, *779*, 138854, https://doi.org/10.1016/j.cplett.2021.138854.
28. Desai, N.D.; Khot, K.V.; Dongale, T.; Musselman, K.P.; Bhosale, P.N. Development of dye sensitized TiO_2 thin films for efficient energy harvesting. *J. Alloys Compd.* **2019**, *790*, 1001–1013, https://doi.org/10.1016/j.jallcom.2019.03.246.
29. Nagmani; Pravarthana, D.; Tyagi, A.; Jagadale, T.C.; Prellier, W.; Aswal, D.K. Highly sensitive and selective H_2S gas sensor based on TiO_2 thin films. *Appl. Surf. Sci.* **2021**, *549*, 149281, https://doi.org/10.1016/j.apsusc.2021.149281.
30. Xu, H.; Huang, W.; Chen, Y.; Liu, Z.; Shen, X.; Zhang, J.; Zhu, X. Fabrication of TiO_2 nanowire array on Ti-4Al-0.005B alloy applied to supercapacitor electrodes. *Chem. Phys. Lett.* **2019**, *732*, 136656, https://doi.org/10.1016/j.cplett.2019.136656.
31. Ahmed, F.; Pervez, S.A.; Aljaafari, A.; Alshoaibi, A.; Abuhimd, H.; Oh, J.; Koo, B.H. Fabrication of TiO_2-Nanotube-Array-Based Supercapacitors. *Micromachines* **2019**, *10*, 742, https://doi.org/10.3390/mi10110742.
32. Riaz, S.; Ashraf, M.; Hussain, T.; Hussain, M.T.; Younus, A. Fabrication of Robust Multifaceted Textiles by Application of Functionalized TiO_2 Nanoparticles. *Colloids Surf. A Physicochem. Eng. Asp.* **2019**, *581*, 123799, https://doi.org/10.1016/j.colsurfa.2019.123799.
33. Li, X.; Yang, H.; Lv, K.; Wen, L.; Liu, Y. Fabrication of porous TiO_2 nanosheets assembly for improved photoreactivity towards X3B dye degradation and NO oxidation. *Appl. Surf. Sci.* **2020**, *503*, 144080, https://doi.org/10.1016/j.apsusc.2019.144080.

34. Kumar, A.; Choudhary, P.; Kumar, A.; Camargo, P.H.C.; Krishnan, V. Recent Advances in Plasmonic Photocatalysis Based on TiO_2 and Noble Metal Nanoparticles for Energy Conversion, Environmental Remediation, and Organic Synthesis. *Small* **2022**, *18*, 2101638, https://doi.org/10.1002/smll.202101638.
35. Stroe, M.; Burlanescu, T.; Paraschiv, M.; Lőrinczi, A.; Matei, E.; Ciobanu, R.; Baibarac, M. Optical and Structural Properties of Composites Based on Poly(urethane) and TiO_2 Nanowires. *Materials* **2023**, *16*, 1742, https://doi.org/10.3390/ma16041742.
36. Qi, Y.; Zeng, X.; Xiao, L.; Li, X.; Liao, H.; Xu, Q.; Xu, J. An invisible hand: Hydrogen bonding guided synthesis of ultrathin two-dimensional amorphous TiO_2 nanosheets. *Sci. China Mater.* **2022**, *65*, 3017-3024, https://doi.org/10.1007/s40843-022-2097-2.
37. Uesugi, Y.; Nagakawa, H.; Nagata, M. Highly Efficient Photocatalytic Degradation of Hydrogen Sulfide in the Gas Phase Using Anatase/TiO_2(B) Nanotubes. *ACS Omega* **2022**, *7*, 11946-11955, https://doi.org/10.1021/acsomega.1c07294.
38. Devi, C.; Swaroop, R.; Arya, A.; Tanwar, S.; Sharma, A.L.; Kumar, S. Fabrication of energy storage EDLC device based on self-synthesized TiO_2 nanowire dispersed polymer nanocomposite films. *Polym. Bull.* **2022**, *79*, 4701-4719, https://doi.org/10.1007/s00289-021-03737-3.
39. Astinchap, B.; Laelabadi, K.G. Effects of substrate temperature and precursor amount on optical properties and microstructure of CVD deposited amorphous TiO_2 thin films. *J. Phys. Chem. Solids* **2019**, *129*, 217–226, https://doi.org/10.1016/j.jpcs.2019.01.012.
40. Astinchap, B.; Ghanbaripour, H.; Amuzgar, R. Multifractal study of TiO_2 thin films deposited by MO-CVD method: The role of precursor amount and substrate temperature. *Optik* **2020**, *222*, 165384, https://doi.org/10.1016/j.ijleo.2020.165384.
41. Tański, T.; Matysiak, W.; Kosmalska, D.; Lubos, A. Influence of calcination temperature on optical and structural properties of TiO_2 thin films prepared by means of sol-gel and spin coating. *Bull. Polish Acad. Sci. Tech. Sci.* **2018**, *66*, 151–156, https://doi.org/10.24425/119069.
42. Paul, T.C.; Podder, J.; Babu, M.H. Optical constants and dispersion energy parameters of Zn-doped TiO_2 thin films prepared by spray pyrolysis technique. *Surf. Interfaces* **2020**, *21*, 100725, https://doi.org/10.1016/j.surfin.2020.100725.
43. Zarhri, Z.; Avilés Cardos, M.Á.; Ziat, Y.; Hammi, M.; El Rhazouani, O.; Cruz Argüello, J.C.; Avellaneda Avellaneda, D. Synthesis, structural and crystal size effect on the optical properties of sprayed TiO_2 thin films: Experiment and DFT TB-mbj. *J. Alloys Compd.* **2020**, *819*, 153010, https://doi.org/10.1016/j.jallcom.2019.153010.
44. Salman, S.H.; Shihab, A.A.; Elttayef, A.-H.K. Design and Construction of Nanostructure TiO2 Thin Film Gas Sensor Prepared by R.F Magnetron Sputtering Technique. *Energy Procedia* **2019**, *157*, 283–289, https://doi.org/10.1016/j.egypro.2018.11.192.
45. Singh, K.J.; Sahni, M.; Rajoriya, M. Study of Structural, Optical and Semiconducting Properties of TiO_2 Thin Film deposited by RF Magnetron Sputtering. *Mater. Today Proc.* **2019**, *12*, 565-572, https://doi.org/10.1016/j.matpr.2019.03.099.
46. Rodrigues, B.V.M.; Dias, V.M.; Fraga, M.A.; da Silva Sobrinho, A.S.; Lobo, A.O.; Maciel, H.S.; Pessoa, R.S. Atomic layer deposition of TiO_2 thin films on electrospun poly (butylene adipate-co-terephthalate) fibers: Freestanding TiO_2 nanostructures via polymer carbonization. *Mater. Today Proc.* **2019**, *14*, 656-662, https://doi.org/10.1016/j.matpr.2019.02.003.
47. Go, D.; Lee, J.; Shin, J.W.; Lee, S.; Kang, W.; Han, J.H.; An, J. Phase-gradient atomic layer deposition of TiO_2 thin films by plasma-induced local crystallization. *Ceram. Int.* **2021**, *47*, 28770-28777, https://doi.org/10.1016/j.ceramint.2021.07.037.
48. Hossain, M.F.; Pervez, M.S.; Nahid, M.A.I. Influence of film thickness on optical and morphological properties of TiO_2 thin films. *Emerg. Mater. Res.* **2020**, *9*, 186-191, https://doi.org/10.1680/jemmr.17.00085.
49. Komaraiah, D.; Radha, E.; Reddy, M.V.R.; Kumar, J.S.; Sayanna, R. STRUCTURAL, OPTICAL PROPERTIES AND PHOTOCATALYTIC ACTIVITY OF NANOCRYSTALLINE TiO_2 THIN FILMS DEPOSITED BY SOL-GEL SPIN COATING. *i-Manager's J. Mater. Sci.* **2019**, *7*, 28, https://doi.org/10.26634/jms.7.1.15719.
50. Aggarwal, R.; Sharma, N.; Kumar, R. Investigating ions concentration effect on structural and optical characteristics of metal-sulphide's thinfilms for photonic devices. *J. Opt.* **2024**, *53*, 136-144, https://doi.org/10.1007/s12596-023-01095-z.